Effect of Natural Variability of Reinforcement on Static Ultimate Capacity of R/C Containment

M.N. Fardis, A. Nacar
Departement of Civil Engineering, Massachusetts Institute of Technology, Room 1-143, Cambridge, Massachusetts 02139, U.S.A.

The response of a typical steel-lined reinforced concrete containment structure to uniform internal pressure monotonically increasing to failure, is investigated by nonlinear Finite Element analysis. Natural variability of the stress-strain properties of reinforcing bars and of the strength of mechanical splices is identified as the dominant uncertainty controlling the response and the ultimate capacity. To illustrate the effect of the random variation of in-place bars and splices, an analysis is first performed with all rebars having average stress-strain curves and with splices assumed stronger than the bars. Results of this analysis, which was discontinued when wall displacements exceeded 500 mm at an internal pressure equal 3.6 times the design value, suggest an ultimate capacity close to 4,25 times the design pressure. A more realistic analysis is also performed, in which the spatial variation of the stress-strain curves of steel bars and of the splice strengths is considered in approximation, by means of "effective"stress-strain laws of the reinforcement. These latter laws, which are developed by simulation using probabilistic models of the stress-strain relation at the generic point of a bar and of the strength of splices, incorporate the effect of progressive failures of bars and splices. This second more realistic analysis predicts ultimate failure at approximately 2,98 the design pressure. In both analyses the critical region is the middle third of the cylinder in the hoop direction. Close to failure this critical region carries the applied pressure by membrane action alone. As a result,the ultimate capacity can be estimated by equilibrium of the membrane forces in the radial direction, provided that the "effective" ultimate strength of the hoop bars is used in the calculation. As this "effective" strength is very close to the average yield stress of the rebars, the latter stress can be used to calculate the ultimate capacity with very little loss in accuracy. The very significant effect of progressive bar and splice failures implies that scale model tests may not be representative of the ultimate behavior of actual concrete structures, unless the natural variability of bars and splices is reproduced in the model.

1. Introduction

The main purpose of the containment structure is to prevent large radio-active release in the event of a serious loss-of coolant-accident. Although limited release may take place due to local loss of leak-tightness, e.g. around penetrations or at the wall-base junction, failure of the containment to fulfill its role can be identified only with gross loss of structural integrity, due to rupture of the reinforcing or prestressing steel, which is the containment's main strength element. Therefore, estimation of the ultimate capacity of a R/C containment structure requires knowledge of the mechanical behavior of the reinforcement, and the uncertainty therein.

There is significant variation of steel properties from bar to bar, and even from point to point of single bar. In addition, the mechanical splices every 18,30 m (60 ft) along each bar have random strength. This natural variability of the rebars and the splices is generally neglected, and the analysis is done assuming average material properties. Due to the very large number of bars in the containment, such an approach is satisfactory for linear or even slightly nonlinear behavior. However, it becomes inadequate when some bars with low strength or ductility start failing, and their load is redistributed to others. Then a more realistic representation of the natural variability of reinforcement becomes necessary. Accounting exactly for it is impractical, due to the cost of the three-dimensional analysis required and the lack of information regarding the actual spatial variation of rebars and splices. Therefore the random steel and splice variation is incorporated in the present analysis in approximation, by means of deterministic "effective"stress-strain relations of the reinforcement, obtained on the basis of simple mechanical assumptions and of local averaging of bar failures.

2. Containment Description and Model

The containment analyzed is an actual steel-lined R/C structure, consisting of a 1,35 m thick cylindrical wall capped with a 1,05 m thick hemispherical dome and supported on a 2,75 m thick base mat. The wall is reinforced with layers of Grade 60 (nominal yield strengh 413 MPa) large diameter (mostly No. 18 and No. 14, i.e. 57 or 44 mm) bars. Hoop reinforcement percentages are 2,1% in the cylinder and 1,2% in the dome,whereas the meridional reinforcement ratio decreases from 2,5% at the lower sixth of the cylinder to 1,25% over the top two-thirds, extending into the dome along meridians. Half of the dome meridional reinforcement is cut off, whenever its percentage becomes twice the required value (at 30^0, $14,5^0$, etc. from the apex). In-plane seismic reinforcement is provided by helical bars at $\pm 45^0$ with the horizontal, at a 0,35% percentage in each direction over the lower three-quarters of the cylinder reduced gradually to zero at the lower third point of the dome. Bars at $\pm 45^0$ with the vertical, within radial planes provide radial shear strength at the lower sixth of the cylinder.

Penetrations are neglected in the analysis and the containment is modeled with axisymmetric 4-noded ring elements for the concrete and 2-noded axisymmetric membrane elements for the layers of reinforcement and for the steel liner. Concrete is considered as a no-tension material and its Modulus is set equal to zero in the directions of positive normal strain (open cracks). The shear slip which accompanies shear transfer across cracks is included, by appropriate definition of the concrete shear rigidity as a function of the amount and stress of the rebars crossing the crack and of the crack spacing. The liner material is considered thermoelastic-perfectly plastic, following the von Mises yield criterion and the associated flow rule. According to the results of field tests on samples of the liner, its uniaxial yield strength is 330 MPa, i.e. 50% higher than the nominal. Finally, the base mat is assumed rigid and the containment is considered fixed at its base. Because the deflection of the mat due to the internal pressure is neglected, the bending-moment at the wall-base junction may be underestimated.

More details about the containment and the Finite Element model are given by Fardis et al. [1].

3. Uncertainty on the Stress-Strain and Strength Properties of Reinforcing Bars

The monotonic σ-ε relation at the generic point of a rebar can be approximated by a linear-elastic region for $\varepsilon \leq \sigma_y/E$ (σ_y = yield strength and E = Young's Modulus), followed by a yield plateau, $\sigma = \sigma_y$, for $\sigma_y/E < \varepsilon \leq \varepsilon_{sh}$ (ε_{sh} = strain at the onset of strain-hardening), and a strain - hardening branch given by

$$\sigma = \hat{\sigma}_u - (\hat{\sigma}_u - \hat{\sigma}_y)\left(\frac{\varepsilon_u - \varepsilon}{\varepsilon_u - \varepsilon_{sh}}\right)^4 \qquad \text{for} \qquad \varepsilon_{sh} < \varepsilon \leq \varepsilon_u \qquad (1)$$

in which $\hat{\sigma}_u$ and ε_u are the stress and strain at ultimate strength (See solid line in Fig.2). One can assume rupture, i.e $\hat{\sigma}$=0, for $\varepsilon > \varepsilon_u$.

Due to inherent variability of the material, differences between the actual cross - sectional area of the bar and the nominal used in the calculations, etc., there is significant varaition of the steel σ-ε curve from point-to-point of a single bar, from bar to bar of the same batch, among batches from the same mill, and from mill to mill. Such variation is treated here as parametric uncertainty on σ_y, σ_u, ε_{sh} and ε_u. (The modulus E has a very small coefficient of variation and is considered here as deterministic quantity equal to 201000 MPa). For simplicity, parameters σ_y, σ_u, ε_{sh} and ε_u are assumed constant along each bar, and independent, identically distributed from bar to bar. Hence, only their joint distribution at each point is required.

The marginal mean and variance of σ_y and σ_u for Grade 60 bars have been estimated by Mirza and MacGregor [2]. The marginal moments of ε_u were obtained from the data by Wiss, Janney and Elstner [3] on elongation at failure, ε_f, and its ratio to ε_u, estimated from the data by Allen [4] on Grade 40 bars. The data by Wiss, Janney and Elstner [3] were also used to estimate the correlation coefficient between σ_y, σ_u and ε_f (and hence ε_u). Finally, the mean and variance of ε_{sh}, as well as its coefficients of correlation with σ_y, σ_u and ε_u were estimated from Allen's [4] data. Table 1 summarizes the second moments of σ_y, σ_u, ε_{sh}, ε_u. The small corre - lation coefficients suggest that within a given steel Grade these 4 parameters are nearly uncorrelated. The data used to estimate the moments support also the assumption that these parameters are jointly Gaussian.

4. Uncertainty on the Strength of Mechanical Splices

In the U.S., T-series Cadweld splices are typically used for bar lengths over 18,3 m (60 ft). According to the ASME-ACI Pressure Vessel Code, any single splice must have strength at least equal to 1,25 the reinforcement nominal yield (i.e. 517 MPa for Grade 60 bars), and every group of 15 consecutively tested splices must have a mean strength at least equal to the specified minimum ultimate strength of the bars (620 MPa for Grade 60 steel). Because the strengths of the splices and the rebars are random, a certain fraction of splices will have strength smaller than that of the bars they connect. Strength data for T-series Grade 60 splices was provided by the splice manufacturer, in the form of compiled field test results and of a testing lab report. In a certain fraction, P_{SF}, of these tests, failure occurred at the splice, whereas in the rest, $1-P_{SF}$, one of the connected bars failed. Calculated sample statistics, conditional on splice failure, are presented in Table 2 and shown in Fig. 1 on Extreme Type I probability paper. Extreme Type I distributions of the smallest values fit well to the conditional-on-splice-failure distribution of strengths. The complementary cumulative distribution function, $G_{S|S.F.}(s)$, of such a distribution is

$$G_{S|S.F.}(s) = P\left[S > s \mid \text{splice fails}\right] = \exp(-\exp\left[a(s-u)\right]) \qquad (2)$$

Values of the dispersion parameter a and of the mode u of the conditional-on-splice-failure distributions are given in Table 2.

5. Effective Stress-Strain Relations of Rebar Ensembles.

The variation of rebar and splice properties is accounted for in approximation by using in the analysis "effective" σ-ε relations for the reinforcement. These relations are based on the probabilistic models described earlier and on certain mechanical assumptions. The development of these "effective" σ-ε models is described next, first for hoops of horizontal bars and then for the meridional and seismic diagonal bars.

Because at large internal pressures horizontal cracks are wide-open and occur preferentially at elevations of hoop bars, it can be assumed that bond stresses along horizontal bars are almost zero, and therefore the rebar force is constant along each hoop. Then, if the σ-ε relation of every bar in the hoop is given (by simulation of the parameters σ_y, σ_u, ε_u and ε_{sh} from their joint distribution), an "effective" stress-average strain curve can be determined for the hoop, by averaging the strains of its m bars at any given value of stress. (Because of the short length of the splices, their deformations contribute insignificantly to the total elongation of the hoop). The peak value ("strength") of the "effective" σ-ε relation is equal to the smallest of 1) the minimum value of σ_u among the m bars, and 2) the minimum strength among the m splices. This latter value is found by simulation from the corresponding complementary cumulative distribution function, $G_{S_{min}}(s)$, which is computed as the probability that the m splices will survive under stress s. For independence of splice strengths this probability equals

$$G_{S_{min}} = P\left[S_{min} > s\right] = \left(P\left[S > s\right]\right)^m = \left(1 - P_{S.F.}\, P\left[S < s|S.F.\right]\right)^m =$$

$$= \left(1 - P_{S.F.}\left[1 - G_{S|S.F.}(s)\right]\right)^m \qquad (3)$$

in which $P_{S.F.}$ = probability that the splice fails before the bar (given in Table 2) and $G_{S|S.F.}(s)$ is given by Eq.(2), with the values of u and a in Table 2. If the simulated value of S_{min} is found less than the lowest among the strengths of the m bars, then it determines the terminal point of the "effective" σ-ε curve of the hoop.

The redistribution of the force of a hoop to neighboring ones, due to rupture of its weakest bar or splice, was investigated by an axisymmetric Finite Element analysis of a 10.65 m high wall segment under uniform internal pressure, after loss of one or two hoops from the interior face at segment midheight. (There is a pair of hoops at each face, at a vertical spacing of 355 mm). It was found that the effect of such hoop losses is not localized to the vicinity of the failed hoop (s), but is felt nearly uniformly by all hoops in the segment. The implication is that the mean circumferential strain in all hoops around a given elevation can be considered the same, regardless of the failure of some hoops. On the basis of this finding and of the high density of bar hoops, an average deterministic "effective" σ-ε relation can be established for the horizontal bars, by considering a large number of hoops— each with a different "effective" σ-ε curve obtained by simulation — as a parallel system with common circumferential strain, and by stress-averaging over all hoops at each given level of strain.

Mechanically spliced meridional and diagonal bars differ from the horizontal ones in that the stress varies in the meridional direction due to bending. To avoid a non-axisymmetric analysis, it is assumed that at a given elevation the meridional strain is constant around the perimeter. Then, an "effective" σ-ε relation is obtained for the meridional and diagonal bars at a single elevation by first simulating the σ-ε curves of all these bars around the perimeter and then stress-averaging at a given meridional strain. The curve so obtained includes the effect of bar failures only at the elevation of interest and neglects what happens at others, e.g. failure at a splice or at the point of maximum meridional strain along the bar, etc,. Such failures can be taken into account only by means of iterative analyses, each time using the maximum strain predicted at each splice elevation and between the elevations of successive splices to estimate the expected number of failures of meridional or seismic diagonal bars, and reduce accordingly the total area of these bars for the next iteration.

"Effective" σ-ε curves for the horizontal reinforcement of the cylinder (8 No. 18 bars per hoop) and for the No. 18 meridional and diagonal bars throughout the structure are compared in Fig. 2 with the σ-ε curve of a single bar with average values of σ_y, σ_u, ε_u and ε_{sh}. "Effective" σ-ε relations for the No. 14 horizontal bars of the dome are shown in Fig. 3, for different numbers of bars perhoop, i.e., for different elevations at the dome. These curves are used as constitutive laws of the 2-noded membrane elements used for the various layers of reinforcement.

6. Results and Discussion.

The containment response to a constant internal temperature of 14D °C and a uniform internal pressure monotonically increasing to failure is obtained by an incremental procedure, firstneglecting splice failures and the variability of steel properties (i.e., using the average values of σ_y, σ_u, ε_u and ε_{sh} everywhere), and second accounting for the variability of bars and splices through the "effective" σ-ε curves of Figs. 2 and 3. In both cases the critical region is found to be the middle third of the cylinder in the hoop direction (Fig.4) Extrapolation of the results of the first analysis suggests an ultimate capacity of approx. 4.25 the design pressure of 324 KPa whereas the second more realistic analysis yield an ultimate capacity of only 2.98 the design pressure. It is also found that the simple expression

$$P = \frac{t_\ell \, \sigma_\ell^h}{R_\ell} + \frac{A_i^h \, \sigma_i^h}{R_i} + \frac{A_o^h \, \sigma_o^h + A_d \, \sigma_d}{R_o} \tag{4}$$

[in which t_ℓ = liner thickness, R_ℓ, R_i, R_o = radius of the liner, the inside and the outside bars, A_i^h, A_o^h = area of inside and outside hoop bars per unit height, A_d = area of diagonal bars in each direction (45^o or - 45^o) per unit length normal to them and σ_i^h , σ_o^h , σ_d = stress in the inside hoop, outside hoop and diagonal bars] gives an ultimate capacity very close to the Finite Element prediction, if one uses in Eq. (4) $\sigma_\ell^h = \frac{2}{\sqrt{3}}$ average uniaxial yield stress of the liner, and $\sigma_i^h = \sigma_o^h \approx \sigma_d$ = "effective"yield strength of spliced hoop bars from Fig. 2. Because the latter value is close to the mean yield strength of Grade 60 bars (460 MPa), using this value for σ_i^h, σ_o^h and σ_d in Eq.(4) results in underestimation of the ultimate capacity by only 2%, compared to an underestimation by 16% when the nominal yield strengths of the bars and the liner are used in the analysis.

In summary, due to progressive failures of bars and splices, the containment does not benefit from the strain hardening and the high average ultimate strength of steel. A realistic estimate of the ultimate capacity can be obtained by considering equilibrium of the membrane forces at cylinder midheight, using the average yield strength of the liner and the steel bars.

ACKNOWLEDGEMENT

The U.S. Nuclear Regulatory Commission, Nuclear Regulatory Research, Mechanical and Structural Engineering Branch, supported this work. Erico Products, Inc., Cleveland, Ohio, United Engineers and Contractors, Philadelphia, Pa, and the Power Authority of the State of New York provided information vital to the study. Valuable discussions with C.Allin Cornell are gratefully acknowledged.

REFERENCES

[1] Fardis, M.N., Nacar, A., and Delichatsios, M.A."Reinforced Concrete Containment Safety under Hydrogen Explosion Loading," Research Report R82-19, Department of Civil Engineering, Massachusetts Institute of Technology, Cambridge, MA, April 1982.

[2] Mirza, S.A., and MacGregor, J.G., "Variability of Mechanical Properties of Reinforcing Bars," Journal of the Structural Division, ASCE, Vol. 105, No. ST5, Proc. Paper 14590, May 1979, p.p. 921-937.

[3] Wiss, Janney, Elstner and Associates, Inc., "Final Report on Bar Tests," for the Committee of Concrete Reinforcing Bars Producers of American Iron and Steel Institute, Northbrook, Ill., Apr. 1970.

[4] Allen, D.E., "Statistical Study of the Mechanical Properties of Reinforcing Bars," Building Research Note No. 85, Division of Building Research, National Research Council of Canada, Ottawa, Canada, Apr. 1972.

Table 1 . Statistics of mechanical properties of Grade 60 bars (Nominal yield 413 MPa)

	Mean	Coeff. of variation %	Correlation Matrix			
σ_y	460 MPa	7	1.0	0.36	-0.12	0.54
σ_u	730 MPa	8	0.36	1.0	-0.36	0.05
ε_u	0.10	21	-0.12	-0.36	1.0	0.10
ε_{sh}	0.01	10	0.54	0.05	0.10	1.0

Table 2 . Strength statistics for Grade 60 T-series Cadweld splices

		No.18	No.14	No.11	No.18 to No.14	No.18 to No.11	No.14 to No.11
Number of tests		1465	523	253	248	87	20
Number of splice failures		655	270	43	49	3	5
Prob. of splice failure, P_{SF}		0,45	0,52	0,17	0,2	0,03	0,25
Mean splice strength, MPa		662	679	665	748	695	695
Max. splice strength, MPa		815	805	786	830	808	817
Min. splice strength, MPa		367	251	408	588	623	632
Stand. deviation, MPa		53	64	71	49	33	52
% above 620 MPa		84,9	90,4	83,7	95,9	100	100
% above 558 MPa		96,2	97,4	90,7	100	100	100
% above 517 MPa		98,8	98,9	97,7	100	100	100
Parameters of fitted extreme Type I distributions	u, MPa	686	727	706	765	-	-
	a	0,168	0,148	0,108	0,151	-	-

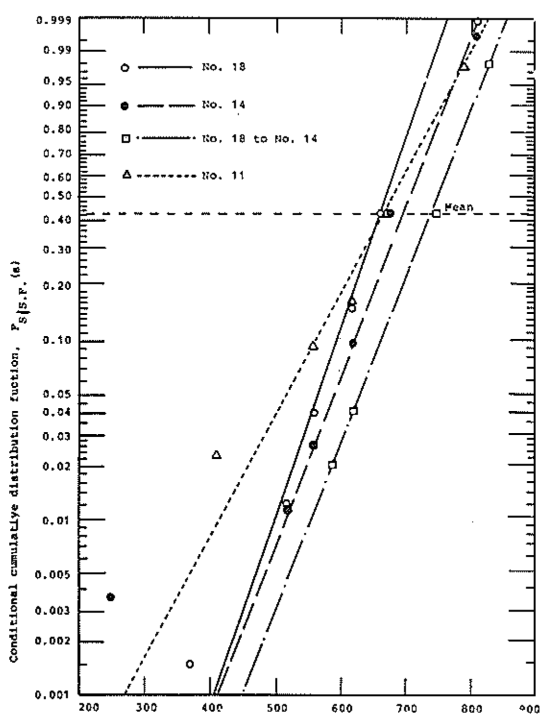

Fig. 1. Conditional-on-splice-failure distribution of splice strengths.

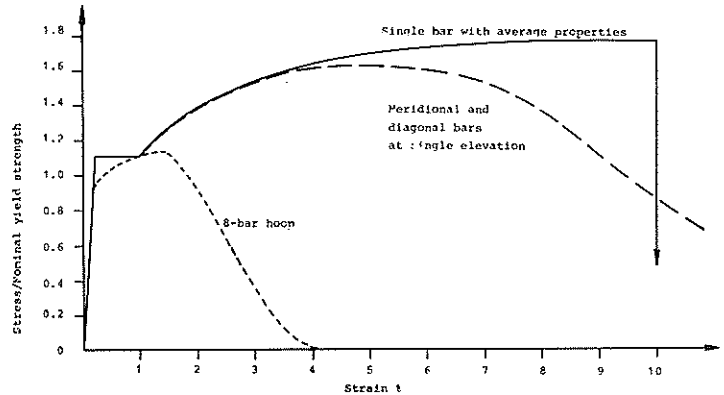

Fig. 2. Effective stress-strain curves of No. 18 rebars, including bar and splice variability.

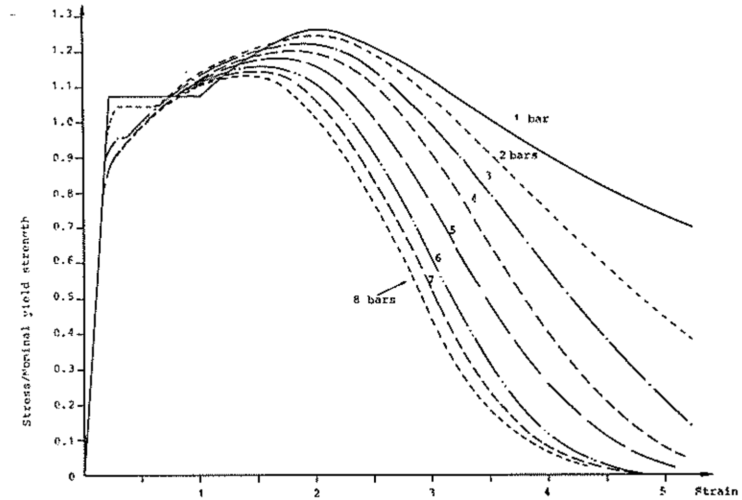

Fig.- 3. Effective stress-strain curves of hoops of mechanically spliced Grade 60, No. 14 bars at the dome.

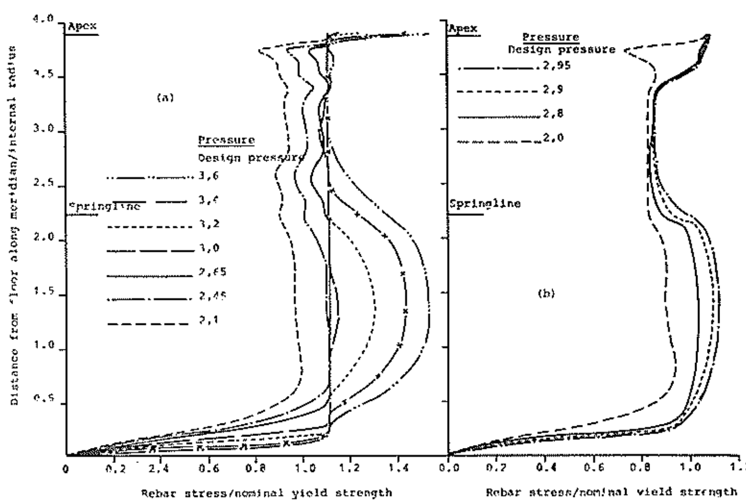

Fig. 4. Stresses of the outside hoop reinforcement. Variability of bar and splices (a) neglected; (b) included

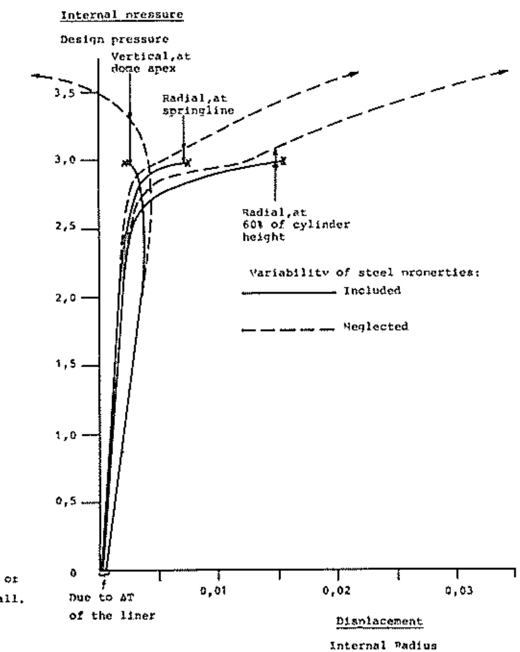

Fig. 5. Displacements of containment wall.